

Relaxation effects in low density amorphous ice: Two distinct structural states observed by neutron diffraction

K. Winkel, D. T. Bowron, T. Loerting, E. Mayer, and J. L. Finney

Citation: *The Journal of Chemical Physics* **130**, 204502 (2009); doi: 10.1063/1.3139007

View online: <http://dx.doi.org/10.1063/1.3139007>

View Table of Contents: <http://scitation.aip.org/content/aip/journal/jcp/130/20?ver=pdfcov>

Published by the AIP Publishing

Articles you may be interested in

Structure and OH-stretch spectroscopy of low- and high-density amorphous ices

J. Chem. Phys. **140**, 134503 (2014); 10.1063/1.4869293

Thermodynamic, structural, and dynamic properties of supercooled water confined in mesoporous MCM-41 studied with calorimetric, neutron diffraction, and neutron spin echo measurements

J. Chem. Phys. **129**, 054702 (2008); 10.1063/1.2961029

Neutron powder diffraction studies of sulfuric acid hydrates. II. The structure, thermal expansion, incompressibility, and polymorphism of sulfuric acid tetrahydrate ($D_2SO_4 \cdot 4D_2O$)

J. Chem. Phys. **128**, 054506 (2008); 10.1063/1.2827474

Neutron powder diffraction studies of sulfuric acid hydrates. I. The structure of sulfuric acid hemitriskaidekahydrate $D_2SO_4 \cdot 6\frac{1}{2}D_2O$

J. Chem. Phys. **125**, 144510 (2006); 10.1063/1.2356860

Structural Relaxation and Low-energy Excitation in Amorphous Ice and Related Glasses

AIP Conf. Proc. **708**, 627 (2004); 10.1063/1.1764240



NEW Special Topic Sections

NOW ONLINE
Lithium Niobate Properties and Applications:
Reviews of Emerging Trends

AIP Applied Physics Reviews

Relaxation effects in low density amorphous ice: Two distinct structural states observed by neutron diffraction

K. Winkel,¹ D. T. Bowron,^{2,a)} T. Loerting,³ E. Mayer,¹ and J. L. Finney⁴

¹*Institute of General, Inorganic and Theoretical Chemistry, University of Innsbruck, A-6020 Innsbruck, Austria*

²*ISIS Facility, Rutherford Appleton Laboratory, Chilton, Didcot, Oxon OX11 0QX, United Kingdom*

³*Institute of Physical Chemistry, University of Innsbruck, A-6020 Innsbruck, Austria*

⁴*Department of Physics and Astronomy, University College London, Gower Street, London WC1E 6BT, United Kingdom*

(Received 2 March 2009; accepted 28 April 2009; published online 26 May 2009)

Neutron diffraction with H/D isotopic substitution is used to investigate the structure of low density amorphous ice produced from (1) high density amorphous ice by isobaric warming and (2) very high density amorphous ice by isothermal decompression. Differences are found in the scattering patterns of the two low density amorphous ices that correlate with structural perturbations on intermediate length scales in the hydrogen bonded water network. Atomistic modeling suggests that the structural states of the two samples may relate to a competition between short range and intermediate range order and disorder. This structural difference in two low density amorphous (LDA) ices is also evident when comparing their compression behavior. In terms of the energy landscape formalism this finding implies that we have produced and characterized the structural difference of two different basins within the LDA-megabasin corresponding to identical macroscopic densities.

© 2009 American Institute of Physics. [DOI: [10.1063/1.3139007](https://doi.org/10.1063/1.3139007)]

One of the intriguing properties of water ice is its ability to exist not only in a number of crystalline phases but also in a number of amorphous forms.^{1–3} These polyamorphs are low density amorphous (LDA) ice,^{4–7} high density amorphous (HDA) ice,^{7,8} and very high density amorphous (VHDA) ice.⁹ Each of these noncrystalline forms is structurally distinct¹⁰ and characterized by a different density ranging from 0.0937 atoms Å^{−3} for LDA, through 0.117 atoms Å^{−3} for HDA, to 0.125 atoms Å^{−3} for VHDA. Since their discovery, the existence of these polyamorphs has become a subject of considerable debate within the context of the general understanding of the physicochemical properties of water, and particularly its liquid state. The low and high density amorphous solids (and since its discovery the very high density form) have been proposed as structural archetypes of low and high density forms of the liquid that, if proven to coexist under appropriate thermodynamic conditions, may relate to some of the scientifically and technologically important characteristics of the water phase diagram.¹¹

From a structural viewpoint, the three amorphous ices are systematically related in terms of the average local coordination of the water molecules.^{12,13} The first shell coordination number of each water molecule goes from ~4 (LDA) to ~5 (HDA) to ~6 (VHDA) neighbors as the density of the ice increases. In all three amorphous solids, each water molecule is on average fully hydrogen bonded to four of its neighbors, with the fifth and sixth neighbors of the higher density structures found in what have been termed interstitial network positions that are themselves also on average thought to be fully hydrogen bonded.^{12,13} Structural anneal-

ing studies of the conversion of the high density forms of ice into the low density forms by heating have been interpreted as suggesting the existence of a family of high density structures,^{14,15} and also the possibility of a range of low density forms.¹⁵ However, this picture has been challenged by subsequent studies^{16–18} that demonstrated that if care is taken to anneal the high density amorphous ice forms to a structure that is thermodynamically metastable with respect to the applied pressure and temperature conditions of ice formation, the complexity of the high density to low density transition is simplified. Subsequently, the annealed form of HDA has been relabeled expanded HDA (eHDA).¹⁷

In a recent computer simulation study of polyamorphism in water,³ the tantalizing possibility of a second distinct low density form of amorphous ice was raised. This challenges the prevailing experimental view of one low density amorphous structure¹⁰ which is thought to be the metastable minimum structure. Within the framework of the simulation, a form labeled LDA_I was produced by warming the model of HDA, while a second slightly more dense ice, LDA_{II}, was produced by warming the model of VHDA. Although interesting, these findings proved to be at odds with existing experimental observations that the density of LDA produced by warming either eHDA or VHDA samples was found to be the same at 0.0937 atoms Å^{−3}.^{1,2}

Although diffraction experiments have so far not been able to elucidate structural differences in differently relaxed LDA states, an unusual observation was recently noted during compression studies of the LDA to HDA transition undertaken in Innsbruck. It was found that the LDA to HDA transformation is slightly sharper and shifted to higher pressure by 0.02 ± 0.005 GPa when the LDA starting point was

^{a)}Electronic mail: daniel.bowron@stfc.ac.uk.

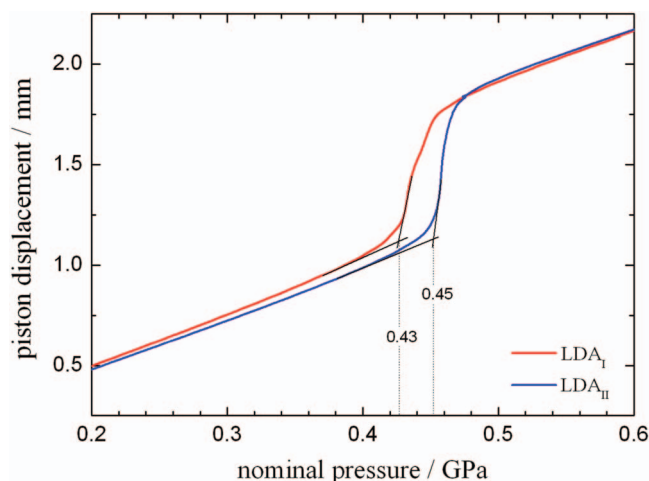


FIG. 1. (Color) Piston displacement curves for isothermal compression of two LDAs produced from HDA and VHDA, both recorded at 125 K with a compression rate of 20 MPa/min. The red curve shows the compression of LDA_I originally obtained by annealing HDA (Ref. 8) at 0.02 GPa to 140 K. The blue curve shows the compression of LDA_{II} originally obtained by decompression of VHDA at 140 K to 0.02 GPa (Ref. 18). All measurements were done with a computerized universal material testing machine (Zwick, model BZ100/TL3S), with a positional reproducibility of 0.5 μm and a spatial resolution of 0.01 μm , in a piston-cylinder apparatus of 10 mm bore diameter. The sample volume is 300 μl of de-ionized water (H_2O). To avoid sudden pressure drops during the measurements, all samples were kept in an indium container. Comparing the LDA_I and LDA_{II} measurements, the onset of the LDA/HDA transformation shifts toward higher pressure by (0.02 ± 0.005) GPa. The transformation of LDA_{II} to HDA also seems to be slightly sharper than in the LDA_I case.

produced from a VHDA ice source rather than from a HDA source (Fig. 1). To achieve this accuracy in the compression experiment, the curves compared were obtained in a single cycle. First a sample of LDA produced from HDA was compressed at 125 K (Fig. 1, red curve). Once data for the first compression curve had been collected, the sample was further compressed to produce VHDA. This VHDA sample was then isothermally decompressed through the eHDA state at 140 K to produce a second LDA sample¹⁸ from which the second compression curve was obtained at 125 K (Fig. 1, blue curve). The complete experimental cycle can thus be summarized as LDA_{HDA} \rightarrow HDA \rightarrow VHDA \rightarrow HDA \rightarrow LDA_{VHDA} \rightarrow HDA, where the subscripts indicate the history of maximum density experienced by the LDA samples. By measuring both curves in this single cycle and avoiding the need to reset the piston cylinder, the reproducibility of the experiment is much better than ± 0.01 GPa.¹⁹ The effect has been measured in three different H_2O -samples and is also found to be visible in D_2O -samples. The behavior suggests the possibility of a structural difference between the two low density amorphous ice forms. Alternatively, the effect may be caused by different strain levels in the amorphous ice samples. Such differences in strain energy may have their origin in the atomistic structure rather than simply being the result of purely mechanical effects.

To investigate in detail the structural relationship between LDA_I and LDA_{II}, adopting the labels assigned in the simulation study,³ we have performed a series of neutron scattering experiments in which we use H/D isotopic substitution to allow us to access the three partial pair distribution

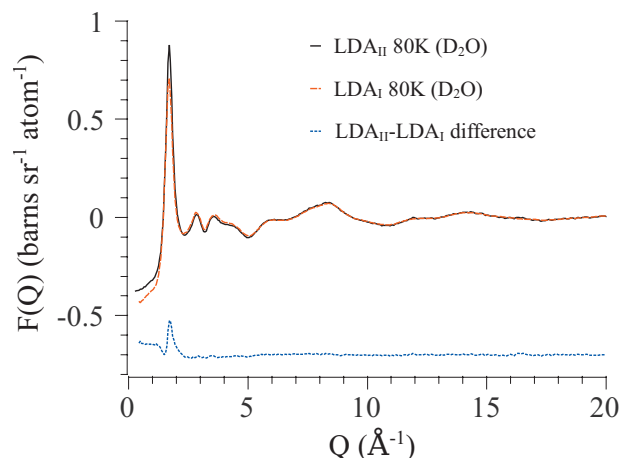


FIG. 2. (Color) Comparison of the LDA_I (broken red line) and LDA_{II} (solid black line) interference differential scattering cross sections, $F(Q)$, measured by neutron scattering from the D_2O ice samples. Q is the magnitude of the momentum transfer during the scattering of the neutron and is defined as $Q = (4\pi/\lambda)\sin\theta$ where 2θ is the scattering angle and λ is the wavelength of the incident neutron. The difference function (dotted blue line) shows that the scattering differences between the two samples are localized in the Q -range of the first diffraction peak. This corresponds to structural differences in the intermediate range beyond 5 \AA . The magnitude of the statistical error bar on these functions is of the order of the thickness of the lines.

functions that characterize the structure of the amorphous solid, $g_{\text{OO}}(r)$, $g_{\text{OH}}(r)$, and $g_{\text{HH}}(r)$. Samples of LDA_I and LDA_{II} were prepared from H_2O , D_2O , and HDO .²⁰ Following the experimental protocols established in our earlier neutron scattering studies^{10,12,13} the amorphous ice samples were loaded into flat plate TiZr cells for data collection at 80 K on the SANDALS diffractometer of the ISIS pulsed spallation neutron source. Each of the isotopic samples used in these measurements had previously been checked for structural equivalence by x-ray diffraction and the isotopic compositions of the D_2O and HDO samples were determined by IR spectroscopy to be 99.9% and 48.5% D, respectively.

Figure 2 illustrates the observed difference in the neutron scattering patterns of the D_2O isotopic samples of LDA_I and LDA_{II}. Clearly, the difference is localized to the Q -region below 2.5 \AA^{-1} , and, in particular, is associated with a change in the height and shape of the first diffraction peak. This prominent feature in the scattering pattern is known to correlate with intermediate range structural organization in liquids and glasses and the difference between the two samples suggests that there are some subtle differences in the topology of the hydrogen bonded network structure of the two low density ices.

The observed difference between the measured $F(Q)$ is considerably larger than the statistical uncertainty of the experimental data, and is thus clearly indicative of the fact that the two ice forms are not structurally identical. However, noting that the strength of the neutron scattering technique is the absolute nature of the measurements, we can immediately conclude, from the highly comparable higher- Q behavior of the interference differential scattering cross sections, that the short range structural correlations in the glasses are effectively identical. This is particularly the case with regards to the local coordination numbers of the water molecules, and is consistent with the observation that the two

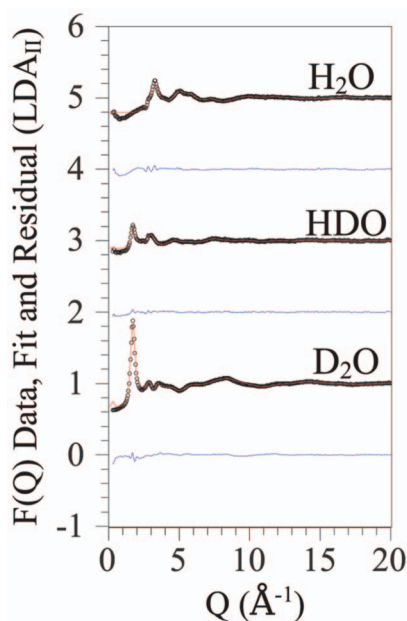


FIG. 3. (Color) The EPSR model fits (solid red line) and fit residuals (dotted blue line) to the D₂O, HDO, and H₂O experimental data (black circles) for LDA_{II}. For clarity the model fits and experimental data are vertically offset by 1.0, 3.0, and 5.0 units, respectively, for the D₂O, HDO, and H₂O samples, while the corresponding fit residuals are vertically offset by 0.0, 2.0, and 4.0 units.

low density ice forms have, within experimental accuracy, the same atomic density.

To investigate how the observed difference in the scattering patterns from the two ice forms is manifest in terms of the molecular structure of the glass, we have performed a detailed analysis of the scattering data following the method outlined in our earlier structural study of the amorphous ice polyamorphs.¹⁰ The scattering functions have been analyzed using empirical potential structure refinement.²¹ This technique produces three dimensional atomistic models of the ice structures that are consistent with the experimental data. As the density of both the LDA_I and LDA_{II} samples is the same,²² the models used for each ice in the structure refinement consisted of 1800 water molecules placed in a cubic box of side length 38.63 Å. Figure 3 shows the model fits and fit residuals to the experimental data for the isotopic samples of LDA_{II} and noting that as LDA_I is the original form of low density amorphous ice, the corresponding figure for this material is already in literature.¹²

Figure 4 shows the three partial pair distribution functions that characterize the structure of each amorphous solid. Small differences between the two ice structures are apparent in the height and width of the first peak in all three pair distribution functions, although the coordination numbers evaluated from these features are, within experimental error, identical. The first neighbor correlations in LDA_{II} appear to be slightly more disordered than LDA_I, marked by the smaller height and slightly greater width of this feature, while interestingly an examination of $g_{OO}(r)$ in the intermediate structural range from 3.5 to 7.5 Å, that corresponds to second and third neighbor correlations between water molecules, suggests that in this distance range the LDA_{II} network is slightly more ordered than LDA_I. This is indicated

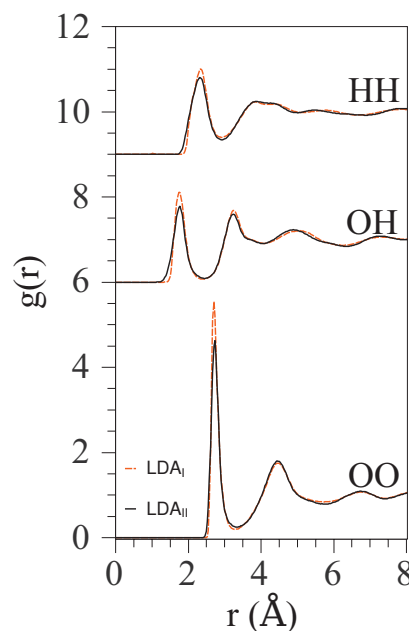


FIG. 4. (Color) Intermolecular partial radial distribution functions of LDA_I (broken red line) and LDA_{II} (solid black line) at 80 K. For clarity, the ordinates for $g_{OH}(r)$ and $g_{HH}(r)$ are shifted by 6 and 9, respectively.

by the second and third neighbor peaks being fractionally sharper for the low density ice produced from the higher density starting material. There thus appears to be a tension between short range disorder and a tendency for intermediate range order in the low density amorphous ice network and suggests one way that the mechanical stresses experienced during the ice formation process may be accommodated within the material.

The scattering data therefore indicate that there exist at least two structural states of low density amorphous ice, where the primary difference in the structures is occurring on an extended length scale in the hydrogen bonded network of molecules. LDA_I and LDA_{II} are not distinct forms of ice in the way that LDA, HDA, and VHDA differ, but rather are two closely related, but kinetically trapped forms of what could be considered the true metastable low density amorphous ice characterized by an atomic density of 0.0937 atoms Å⁻³.

In terms of an energy landscape that is explored during the transition from the high density structures to the lower density state, the two structures can be considered representatives of related but different energy minima in the general LDA energy basin. In order to assess, which of the two minima is lower in terms of enthalpy, we have measured differential scanning calorimetry thermograms of LDA_I and LDA_{II} at 1 bar. These thermograms show a sharp peak corresponding to crystallization (LDA → cubic ice). For LDA_I we had reported the enthalpy of crystallization by integration of this peak as -1.37 ± 0.06 kJ/mol,²³ which is nearly the same as that reported by Handa *et al.* (see Table I in Ref. 24). For LDA_{II} obtained by decompression of VHDA at 140 K to 0.02 GPa we determined two values of -1.32 and -1.31 kJ/mol from the same batch. Thus, LDA_{II} seems to be slightly closer to the metastable equilibrium than LDA_I, which is consistent with the higher stability of LDA_{II} against

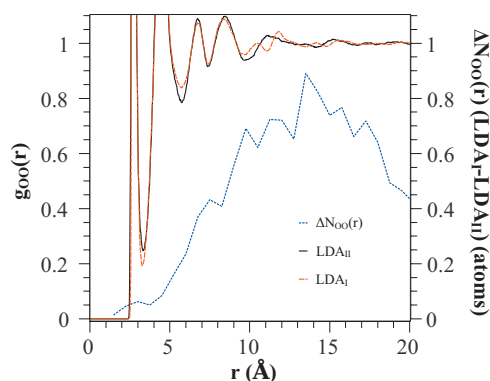


FIG. 5. (Color) Plot of the difference in the relative coordination number of oxygen atoms about the oxygen site of an arbitrarily selected water molecule as a function of radial distance for the LDA_I and LDA_{II} ice networks (blue dotted line). The difference function has been calculated in radial shells of 3 Å thickness (approximately the size of one water molecule). The function indicates that in the shorter <10 Å and longer ≥20 Å distance ranges the number of water molecules in each network are similar, while in the intermediate range about one additional water molecule is packed into the LDA_I network. For clarity, also shown are the oxygen-oxygen partial distribution function for LDA_{II} (black solid line) and LDA_I (red dashed line) over the comparable distance range.

pressure transformation. Judging from the thermal history we also assume LDA_{II} to be a more relaxed state than LDA_I. The difference in structure thus corresponds to a different degree of relaxation of two states of identical density rather than a polyamorphic structural transition. Upon changing the starting material and the p , T conditions for the production of LDA we expect a possible multitude of LDA structures within the LDA megabasin.

Finally, to quantify the relationship between the two low density structures, it is informative to consider the difference in how the water molecules are distributed relative to an arbitrary molecular center over an extended range. This can be shown by plotting the difference between the running coordination number of oxygen atoms in the two ice networks calculated in radial shells of a thickness corresponding to the size of a water molecule (~ 3 Å) (Fig. 5). The running coordination number is defined as

$$N_{\beta}^{(\alpha)}(r) = 4\pi\rho c_{\beta} \int_0^r r'^2 g_{\alpha\beta}(r') dr', \quad (1)$$

where $N_{\beta}^{(\alpha)}(r)$ is the coordination number of atoms of type β about α , ρ is the atomic number density, c_{β} is the concentration of atoms of type β in the system, and $g_{\alpha\beta}(r)$ is the partial distribution function between the two atomic species. This plot shows that within the constraints of the structural model, i.e., that both the LDA_I and LDA_{II} structures are built from identical numbers of water molecules and have the same bulk density, the networks form with very similar numbers of water molecules on the short (first and second neighbors) and long length scales ≥20 Å. However, in the intermediate distance range around 15 Å, the LDA_I network, on

average, packs close to one additional water molecule into the structure. We can speculate that it may be the trapping or otherwise of this additional water molecule during the low density ice formation process that induces the aforementioned tension between short (first neighbor) and intermediate range structural order in the network.

- ¹ P. G. Debenedetti, *J. Phys.: Condens. Matter* **15**, R1669 (2003).
- ² T. Loerting and N. Giovambattista, *J. Phys.: Condens. Matter* **18**, R919 (2006).
- ³ B. Guillot and Y. Guissani, *J. Chem. Phys.* **119**, 11740 (2003).
- ⁴ E. F. Burton and W. F. Oliver, *Nature (London)* **135**, 505 (1935).
- ⁵ A. Hallbrucker, E. Mayer, and G. P. Johari, *J. Phys. Chem.* **93**, 7751 (1989).
- ⁶ E. Mayer and P. Brüggeller, *Nature (London)* **288**, 569 (1980).
- ⁷ O. Mishima, L. D. Calvert, and E. Whalley, *Nature (London)* **314**, 76 (1985).
- ⁸ O. Mishima, L. D. Calvert, and E. Whalley, *Nature (London)* **310**, 393 (1984).
- ⁹ T. Loerting, C. Salzmann, I. Kohl, E. Mayer, and A. Hallbrucker, *Phys. Chem. Chem. Phys.* **3**, 5355 (2001).
- ¹⁰ D. T. Bowron, J. L. Finney, A. Hallbrucker, I. Kohl, T. Loerting, E. Mayer, and A. K. Soper, *J. Chem. Phys.* **125**, 194502 (2006).
- ¹¹ O. Mishima and H. E. Stanley, *Nature (London)* **396**, 329 (1998).
- ¹² J. L. Finney, A. Hallbrucker, I. Kohl, A. K. Soper, and D. T. Bowron, *Phys. Rev. Lett.* **88**, 225503 (2002).
- ¹³ J. L. Finney, D. T. Bowron, A. K. Soper, T. Loerting, E. Mayer, and A. Hallbrucker, *Phys. Rev. Lett.* **89**, 205503 (2002).
- ¹⁴ C. A. Tulk, C. J. Benmore, J. Urquidí, D. D. Klug, J. Neuefeind, B. Tomberli, and P. A. Egelstaff, *Science* **297**, 1320 (2002).
- ¹⁵ M. M. Koza, H. Schober, H. E. Fischer, T. Hansen, and F. Fujara, *J. Phys.: Condens. Matter* **15**, 321 (2003).
- ¹⁶ O. Mishima and Y. Suzuki, *Nature (London)* **419**, 599 (2002).
- ¹⁷ R. J. Nemes, J. S. Loveday, T. Strässle, C. L. Bull, M. Guthrie, G. Hamel, and S. Klotz, *Nat. Phys.* **2**, 414 (2006).
- ¹⁸ K. Winkel, M. S. Elsaesser, E. Mayer, and T. Loerting, *J. Chem. Phys.* **128**, 044510 (2008).
- ¹⁹ The accuracy that can be obtained when comparing two separate experiments is about ± 0.01 GPa and is much better when comparing two curves in a single experiment. The accuracy of the compression curve measurements has recently been improved beyond the original method reported in K. Winkel, W. Schustereder, I. Kohl, C. G. Salzmann, E. Mayer, and T. Loerting, Proceedings of the 11th International Conference on the Physics and Chemistry of Ice, 2007, pp. 641–648. This improvement was achieved by (i) reducing the height of the sample through the use of a 10 mm bore compression volume instead of the original 8 mm bore, (ii) by carefully controlling the history of the LDA sample (e.g., annealing time, temperature, rate of and heating) and (iii) by improving the temperature control of the sample from ± 2 K to ± 1 K at all stages of the transformation.
- ²⁰ LDA_I was produced by controlled heating of HDA to 122 K and recooling to 80 K directly in the TiZr cell during the neutron scattering experiment (Ref. 12). LDA_{II} was produced in a piston-cylinder apparatus of 10 mm bore diameter by slow decompression of VHDA at 140 K to 0.02 GPa with a rate of 20 MPa/min, and then quench recovering the sample (Ref. 18). The original VHDA state was prepared via the formation of HDA by the compression of hexagonal ice at 100 K to a pressure of 1.4 GPa (Refs. 7 and 17), followed by annealing at 1.1 GPa to 160 K.
- ²¹ A. K. Soper, *Phys. Rev. B* **72**, 104204 (2005).
- ²² The density of both LDA_I and LDA_{II} is the same and had been measured by flotation as described in Ref. 10.
- ²³ C. G. Salzmann, I. Kohl, T. Loerting, E. Mayer, and A. Hallbrucker, *Phys. Chem. Chem. Phys.* **5**, 3507 (2003).
- ²⁴ Y. P. Handa, O. Mishima, and E. Whalley, *J. Chem. Phys.* **84**, 2766 (1986).